Supplementary Material

Comparing HVAC Energy-Saving Measures in a Saudi Residential Building under a Volume Tariff

Anonymised for double-blind review

This supplementary material accompanies the manuscript of the same title. Sections, tables, figures and equations numbered with the prefix S are in this document; those without it are in the manuscript. References are numbered as in the manuscript.

S1 Nomenclature

Table S1 lists the symbols used in more than one section.

S2 Proofs

Proof of Theorem 1. Over one period T of the cycle the stored heat returns to its initial value, so the heat removed equals the heat gained: $\int_0^T f_m \psi Q_i \mathbb{1}_{\text{on}}\, dt = \int_0^T L(V(t))\, dt$. With the outdoor conditions and the neighbours' levels constant (A3, A4), $L(V) = a - bV$ is affine with $b \geq K_i^{\text{env}} + K_i^{\text{grd}} > 0$ (b also contains the conductances to passive neighbours), so $\int_0^T L(V(t))\, dt = T\, L(\bar{V})$. The door exchange with a warmer passive zone j, $q_{ji} \propto (V_j - V_i)^{3/2}$ by Eq. (3), is convex in V_i; with it L is convex, Jensen's inequality gives $\int_0^T L(V(t))\, dt \geq T\, L(\bar{V})$, and Eq. (8) becomes a lower bound whose error is of second order in the amplitude. The electrical energy of the cycle is the heat removed divided by COP_m, and dividing by T gives Eq. (8). (i) For a cycle between $V_{\text{high}} - \Delta$ and V_{high} both legs are exponential and, to first order in Δ, linear in time, so $\bar{V} = V_{\text{high}} - \Delta/2$. The numerator of Eq. (8) decreases with the level: when every conditioned zone is raised by $\mathrm{d}\bar{V}$ (A4), the exchange with conditioned neighbours is unchanged, each passive zone, whose monthly mean temperature is by its heat budget (Section S6) a weighted mean of its neighbours' and the outdoor and ground temperatures, rises by at most $\mathrm{d}\bar{V}$, and the envelope and ground inflows fall by $(K_i^{\text{env}} + K_i^{\text{grd}})\, \mathrm{d}\bar{V}$; hence $\mathrm{d}L/\mathrm{d}\bar{V} \leq -(K_i^{\text{env}} + K_i^{\text{grd}}) < 0$. The denominator decreases with the mode, since $c_1 > c_2 > c_3$. Hence $\bar{P}$ is minimised by the highest admissible level and, at that level, by the lowest mode that holds the room; a mode with $f_m \psi Q_i \leq L$ cannot bring the zone back from the top of the cycle, so the zone passes the ceiling. A thermostat with differential Δ_{th} centred on its setpoint cycles between the setpoint $\pm\Delta_{\text{th}}/2$, so its highest admissible setpoint is $V_{\text{high}} - \Delta_{\text{th}}/2$, which is also its level. (ii) With constant ambient conditions, integrating the heat balance of an arbitrary safe infinite schedule over $[0, T]$ gives the heat removed as $\int_0^T L(V(t))\, dt$ plus a change in stored heat that stays bounded because V stays in the safe set. Dividing by T and letting $T \to \infty$, the long-run mean heat removed equals the long-run mean of $L(V(t))$, at least $L(V_{\text{high}})$ because L decreases with V and $V \leq V_{\text{high}}$. At every instant the unit is off or in one mode, so its power is at least $\check{P}$ of its heat removal; since $\check{P}$ is convex and non-decreasing, Jensen's inequality bounds the long-run mean power below by $\check{P}$ of the long-run mean heat removal, which is at least $\check{P}\big(L(V_{\text{high}})\big)$. Because COP_m falls with m, the chord from the origin to mode m has slope $1/\text{COP}_m$, the least for $m = 1$, so the first piece of $\check{P}$ joins the origin to mode 1 and $\check{P}(L) = L/\text{COP}_1$ for $L \leq f_1 \psi Q_i$. In that range mode-1 cycles at the ceiling approach the bound as $\Delta \to 0$ by (i). For $L > f_1 \psi Q_i$, a schedule that alternates at the ceiling between the two vertices of $\check{P}$ bracketing L, in the proportions that remove L on average, attains $\check{P}(L)$ in the limit of vanishing amplitude, and $\check{P}(L) < L/\text{COP}_{m^*}$ unless $L = f_{m^*} \psi Q_i$ or the vertex below L is the origin. When mode 1 holds the room, with a given differential no schedule holds a higher mean than the optimal leap, and any schedule that holds the zone below $\bar{V}^*$ for a positive fraction of time raises the mean of $L(V(t))$ and therefore J_∞. □

Proof of Corollary 1. By Eq. (8) the mean power of each zone is fixed by its level and mode (or mix of modes on $\check{P}$); summing over zones and time gives the cost, in which neither the number of cycles nor the assignment of heat to units appears. The PLF rises with the runtime fraction $L/(f_m \psi Q_i)$, which is largest in the lowest mode. □

Proof of Proposition 1. Over a periodic cycle the heat removed equals the heat gained (the coupling between conditioned zones held at a common level cancels under (A4), Section 6.1). Pre-cooling lowers V_i for part of the cycle, so the zone gains $\Delta H \geq 0$ more heat, and because the ceiling is hard it cannot compensate by rising above V_{high} later. In the window the unit removes $C_i \delta$ plus the part $\Delta H_w \geq 0$ of the extra heat admitted there, at the incremental COP_w, which costs $(C_i \delta + \Delta H_w)\eta_w$; later it removes $C_i \delta - \Delta H_r \geq 0$ less, with $\Delta H_r = \Delta H - \Delta H_w \geq 0$, at an incremental COP of at least COP_p, which saves at most $(C_i \delta - \Delta H_r)\eta_p$. Hence $\Delta E \geq C_i \delta(\eta_w - \eta_p) + \Delta H_w \eta_w + \Delta H_r \eta_p$, and bounding both coefficients below by $\min(\eta_w, \eta_p)$ gives Eq. (9). □

Proof of Proposition 2. By Eq. (5) the bill depends on the policy only through the meter energies $E_{r,k}$, each the heat removed by the meter's units in month k divided by their mean effective COP, so the timing of the leaps within a month matters only through these two quantities. By Theorem 1, applied hour by hour to the level at which a zone is held (which requires (A3), so that for long cycles this step is an approximation), each unit's mean power, and hence each meter's energy, decreases as its level rises. A bill that is non-decreasing in every $E_{r,k}$ is therefore minimised at the highest level allowed by (C2), $\bar{V}^*$; this is (i). By Proposition 1, any $\delta_{\text{night}} > 0$ or $\delta_{\text{peak}} > 0$ that satisfies its no-gain condition

Table S1 Nomenclature.

Symbol	Meaning	Symbol	Meaning
$\mathcal{Z}, \mathcal{Z}_c, \mathcal{Z}_u$	zones; conditioned; passive	V_i; W_i	air; structure temperature of zone i [°C]
C_i; $C_i^{\mathrm{a}}, C_i^{\mathrm{m}}$	thermal capacitance; its air and structure parts [kWh/K]	K_i^{env}	zone–outdoor conductance [kW/K]†
$K_i^{\mathrm{w}}, K_i^{\mathrm{o}}$	window and infiltration; opaque conductance [kW/K]	K_i^{am}	air–structure conductance [kW/K]
$S_i^{\mathrm{o}}, S_i^{\mathrm{w}}, S_i^{\mathrm{sky}}$	opaque sol-air, window solar, window sky drives [kW]	f_r; β_i	radiant share of gains; run fraction of a step
K_{ij}	coupling conductance of zones i, j [kW/K]	K_i^{grd}	zone–ground conductance [kW/K]
G_i	internal gains [kW]	L	heat gain of a zone [kW]
q_i^{env}	heat entering via envelope and ground [kW]	q_{ji}	heat carried through a door [kW]
M, m	mode set $\{0, 1, 2, 3\}$; a mode	f_m	capacity fraction of mode m
Q_i; Q_i^{h}	cooling; heating capacity of unit i [kW]	COP_m	coefficient of performance
ψ; g, γ	capacity derating with T_a; indoor COP factor, its slope [K^{-1}]	C_d; PLF; RTF	cycling degradation; part-load factor; runtime fraction
(m, t)	timed action: mode m for time t	Δ; Δ_{th}	amplitude of a leap cycle; thermostat differential [K]
σ	schedule (finite or infinite)	$\pi_i(m)$	cost per unit time, unit i, mode m
θ^*	selected policy (frontier setpoint, best depths)	λ	energy price [SAR/kWh]
$\bar{V}$; $\bar{V}^*$	level (time-mean temperature) of a leap cycle; highest admissible level (comfort frontier)	U; d_m	utilisation; duty in mode m
$[V_{\mathrm{low}}, V_{\mathrm{high}}]$	comfort band $[22, 24]$ °C	$[V_{\min}, V_{\max}]$	safe set $[20, 24]$ °C
θ	policy $(V^{\mathrm{cool}}, V^{\mathrm{heat}}, \delta_{\mathrm{night}}, \delta_{\mathrm{peak}})$	$E_{r,k}$	energy of meter r in month k [kWh]
Π	annual bill [SAR]	T_a, T_g	outdoor, ground temperature [°C]
$u_i(t)$; $s_i(t)$	mode of unit i; $+1$ cooling, -1 heating	c_m, h_m; φ	cooling, heating COP coefficients; outdoor COP factor
ω_a, ω^*	outdoor, indoor humidity ratio [g/kg]	n_{ach}	infiltration [air changes per hour]
$\delta = (\delta_{\mathrm{night}}, \delta_{\mathrm{peak}})$	pre-cooling depth pair [K]	U-value	thermal transmittance [W/m^{2}K] (not U_i)
$V^{\mathrm{cool}}, V^{\mathrm{heat}}$	cooling, heating setpoint [°C] (V^{heat} fixed, (C5))	$\mathrm{COP}_{\mathrm{lat}}$	latent (dehumidification) COP
J_∞	long-run mean electrical power [kW]	x_t; q_{it}; $v_{\min}$	nodal temperatures; heat removal; pre-cooling floor (benchmark)
V_0	initial state of a run (not a setpoint)	Π^{vol}	annual bill under the volume tariff [SAR]
$\tilde{P}$	lower convex envelope of a unit's mode power curve [kW]	κ_θ	controller under policy θ, (C0)
$\mathrm{COP}_w, \mathrm{COP}_p$; η_w, η_p	incremental COP in and after the pre-cooling window; their inverses	ΔH; $\Delta H_w, \Delta H_r$	extra heat admitted by pre-cooling; in and after the window [kWh]

†Conductances are quoted in W/K in the running example. Symbols used only locally are defined where they appear.

Table S2 The baths of the SBC-compliant building (Case 3, the whole building; 32 baths) with and without the controller: July mean and annual peak temperature [°C], share of the year above the 24 °C ceiling [%], mean excursion above the ceiling per bath [K·h/yr], and the building's HVAC energy relative to the controller of this study [%].

	Riyadh					Jeddah				
Variant	July	Peak	>24 °C	K·h	Energy	July	Peak	>24 °C	K·h	Energy
No controller (all units off)	41.3	44.3	83	79,141	–	39.3	41.7	99	96,640	–
Controller, interior doors closed	27.7	31.9	68	15,164	+0.1	27.1	31.4	97	18,350	−0.3
Controller, reference setpoint (this study)	24.9	26.3	62	3,509	0	24.7	26.3	91	4,248	0
Controller at current practice (22 °C)	23.5	25.0	6	118	+14.2	23.3	24.9	4	52	+11.7
Controller and a 1-ton unit in every bath	23.6	24.0	0	0	+2.8	23.7	24.0	0	0	+4.9

gives $\Delta E \geq 0$ for every affected meter and so does not lower the bill, and raises it if the tariff is strictly increasing and $\Delta E > 0$. The argument is applied zone by zone: under (A4) the conditioned zones are held at a common level, so the coupling between them carries no net heat (Section 6.1) and a meter's energy is, to that approximation, the sum of its zones' terms; coupling to zones of other meters cancels only in the sum over the building. Where the no-gain condition fails, Proposition 1 gives $\Delta E \geq -C_i\delta(\eta_p - \eta_w)$ for each zone, the stated bound. Nothing in the argument uses the tariff beyond its monotonicity in energy, which is (ii). □

Proof of Proposition 3. By Theorem 1, the mean electrical power of zone i over a cycle is L_i/COP_{u_i}, and summing over cycles and zones gives E. The heat gain L_i decreases as V_i rises and as K_i^{env} falls, and COP_m decreases with m (Eq. (1)). Pre-cooling lowers V_i below the setpoint for part of the day and so raises L_i there (Proposition 1). No other term of E depends on the policy. □

S3 Passive zones with and without the controller

The model imposes the 24 °C ceiling on the conditioned rooms only, and the passive zones exceed it on warm days. Table S2 shows how much of this excursion the controller removes without acting on them (32 baths of the whole building). With every unit off all year the baths average 39.3–41.3 °C in July and peak at 41.7–44.3 °C. With the controller holding their neighbours at the reference setpoint, they average 24.7–24.9 °C in July, and their excursion above the band falls by 96%. They shed their heat to the conditioned neighbours through the walls and, above all, through the open doors (as the heat budget of Section S6 predicts): with the interior doors closed the excursion is 4.3 times larger. A 1-ton unit in every bath would hold them in the band for 2.8–4.9% more energy, and colder neighbours (current practice) would cost 11.7–14.2% more.

Table S3 Rooms of apartment A and the stair core (apartment B mirrors A, with west and east exchanged). Clear size and clear area from the drawing; floor area of the zone as modelled, on wall centrelines (used for capacitance, internal gains and the energy intensity); exterior faces with the widths of their windows [m] (all windows 1.50 m high); split unit, by rated coverage of the clear area; gain factor: multiple of the per-area internal gain given in Table 3. The rooms are the same on every storey; the ground-floor rooms also lose heat to the ground and the top-floor rooms gain it through the roof.

Room	Clear size [m]	Clear area [m^2]	Zone area [m^2]	Exterior faces (windows)	Unit	Gain factor
Master bedroom	5.00×5.00	25.0	27.3	N (2.00), W	2.5 t, inverter	1.0
Bed 2	4.00×4.00	16.0	17.7	N (2.00)	1.5 t, inverter	1.0
Master bath	2.50×1.50	3.8	4.5	W (0.90)	–	0.5
Lobby	2.35×1.50	3.5	4.1	–	–	0.3
Bath 2	2.00×2.00	4.0	4.8	–	–	0.5
Maid room	2.00×2.00	4.0	4.8	–	–	1.0
Corridor	irregular	–	23.0	–	–	0.3
Bed 3	4.00×4.00	16.0	17.5	W (1.80)	1.5 t, inverter	1.0
Balcony (enclosed)	1.50×5.00	7.5	9.3	W (4.00)	–	0.0
Living room	5.00×5.00	25.0	26.9	–	2.5 t, inverter	1.0
Dining area	2.20×5.00	11.0	12.4	–	1.5 t, inverter	1.0
Kitchen	4.00×4.00	16.0	17.5	W (1.80)	1.5 t, inverter	1.5
Hall and entrance	irregular	–	22.9	–	–	0.3
Bath 3	2.00×2.00	4.0	5.0	–	–	0.5
Guest room	6.90×5.00	34.5	37.5	S (2.00), W (2.00)	3.0 t, fixed-speed	1.0
Bath 4	2.00×2.00	4.0	4.8	W (0.80)	–	0.5
Stair and lobby (core)	4.25×9.05	38.5	42.0	S (2.00)	3.0 t, fixed-speed	0.3

S4 Perfect-foresight benchmark on every design day

This appendix summarises the perfect-foresight benchmark of Section 9.3 on every design day solved, in the columns of Table 10, which shows a selection of these rows, and the ranges it quotes are taken over all of them. The $\gamma = 0$ columns are rigorous upper bounds on what any periodic schedule of the idealised model could save; the $\gamma = 0.02$ columns are achievable savings, those of the best valid schedule found by the sequential linear programming of Section 7.2. The search improves on holding the ceiling on 44 of the 48 design-day programs at $\gamma = 0.02$; on the others no valid schedule cheaper than the reference was found. Two checks support the linear model: linearising the door exchange about 0.2 or 1.0 K instead of 0.5 K moves the bound by at most 0.13 percentage points, and the full nonlinear engine, run with ideal equipment holding the ceiling in its lowest mode, differs from the linear model's reference by -3.1 to -0.9%; the schedule and its reference share the linear model, so this error bears on their level more than on the saving.

Every design day. For one apartment (Case 1) the bound within the band on the mean days of May to September is 0.79, 1.05, 1.26, 1.41 and 0.82% in Riyadh and 0.59, 0.87, 0.78, 0.24 and 0.34% in Jeddah, largest in August (Riyadh) and June (Jeddah), and 1.50% in Riyadh and 1.79% in Jeddah on the hottest July day; down to 20 °C it is 0.42–3.34% over these days. The achievable saving found at $\gamma = 0.02$ is 0.01–0.54% both within the band and down to 20 °C. On the three design days of the typical floor (Case 2) the bound is 0.27–1.92% (achievable 0.00–0.63%), under the roof 0.07–1.08% (0.00–0.25%), and for the whole building 0.13–1.34% (bound only), each within the band. Holding the ceiling uses 13.7–25.4 kWh of sensible cooling electricity a day for one apartment, 35.9–53.8 kWh for the typical floor, 43.5–64.5 kWh for the top floor and 157.3–235.6 kWh for the building; the bound is a percentage of this reference.

S5 Building geometry and weather

This appendix gives the room dimensions and the list of rooms of the building and the monthly weather and ground temperature that Sections 4.3 and 4.1 and Fig. 2 summarise.

Room dimensions. Table S3 lists the clear size of every room; the living room is open over its full width to the dining area and joined by a sliding door to the enclosed west balcony. The common stair is 4.25×9.05 m clear. Exterior walls are 0.30 m thick, the party and stair walls 0.25 m and partitions 0.15 m. Windows are 1.50 m high (sill 0.90 m, head 2.40 m), 0.80–2.00 m wide in the rooms and 4.00 m on the balcony. Table S3 lists every room with its zone area as modelled, its exterior faces and windows, its unit and the factor that scales its internal gain.

Weather. The model is driven by the TMYx typical years of Riyadh Air Base (WMO station 404380) and Jeddah King Abdulaziz International Airport (WMO 410240), described in the Data availability statement. Their monthly values (the mean, mean daily maximum and minimum dry-bulb temperature, mean relative humidity, global horizontal irradiation and undisturbed ground temperature at 2 m depth) are plotted in Fig. 2. Beyond the values given in Section 4.1, Riyadh's mean daily maxima exceed 43 °C in July and August, its mean daily minima range from 8.7 °C (January) to 29.4 °C (July), and its relative humidity falls from 47% in winter to 12% in summer; its monthly global irradiation ranges from 4.2 (December) to 7.7 kWh/m^2 per day (June). Jeddah's monthly mean peaks at 33.2 °C in August, its mean daily maxima stay between 28.8 and 39.0 °C, and it receives 4.4–7.4 kWh/m^2 of irradiation per day. The ground temperature under the slab follows the seasons with a lag: from 19.3 °C in January to 33.8 °C in July in Riyadh, and from 25.5 °C in

February to 31.9 °C in August in Jeddah.

S6 Formal definitions and running examples

This appendix states in full the definitions that Section 5 summarises, in the notation of the multi-mode literature cited there [11, 16], and on which the theory of Section 6 rests. The appendix also continues the running example (Bed 2 of apartment 2A) and derives the heat budget of a passive zone.

S6.1 Zones, units and the multi-mode system

Definition S6.1 (Coupled zone network). The zones $\mathcal{Z}$, their conditioned and passive subsets $\mathcal{Z}_c$ and $\mathcal{Z}_u$, the capacitances C_i, the couplings K_{ij} and the envelope conductances K_i^{env} are those of Section 5. Two zones are *adjacent* if $K_{ij} > 0$, and a zone with an exterior wall, window or roof is an *edge zone*. Heat flows from zone j into zone i through shared walls and slabs, at the rate $K_{ij}(V_j - V_i)$, and by buoyant exchange through an open door between them (Eq. (3)), and leaves the building through the edge zones.

Definition S6.2 (Multi-directional multi-mode unit). The unit of a conditioned zone (Section 5) is multi-directional: in mode $m \in M$ it moves heat out of the zone when cooling and into it when heating, with the capacity fractions $0 = f_0 < f_1 < f_2 < f_3 = 1$, and its electricity is the heat moved divided by the cooling or heating COP of Eq. (1). The thermostat decides the direction. For passive zones $f_m Q_i \equiv 0$.

Definition S6.3 (Multi-mode system with costs). Following Mousa et al. [12], the building is a multi-mode system $\mathcal{A} = (\mathbf{M}, N, A, \pi, V_{\min}, V_{\max}, V_0)$. Here $\mathbf{M} = M^{|\mathcal{Z}_c|}$ is the set of mode vectors, one mode per unit; $N = |\mathcal{Z}|$ is the number of continuous variables, the zone temperatures $V = (V_1, \dots, V_N)$; A gives the rate of change of V under each mode vector, which is the heat balance of Eq. (2); $\pi_i(m)$ is the cost per unit time of unit i in mode m, given for the Saudi tariff in Section 5.6; the bounds $V_{\min}$ and $V_{\max}$ define the safe set $\mathcal{S} = [V_{\min}, V_{\max}]$ of the conditioned zones; and V_0 is the initial state.

Remark S6.1. As noted in Section 5.3, the building is close to a linear-rate multi-mode system [15]; when the heat gain is held constant over a short interval (assumption A3) the rates are constant and the theory of Alur et al. [14] applies.

S6.2 Timed actions, schedules, runs and costs

Definition S6.4 (Timed action and leap). A *timed action* is a pair $(m, t) \in M \times \mathbb{R}_{>0}$ of a mode m and a duration t: the unit stays in mode m for time t. A timed action is a *leap* when it moves the zone temperature from one bound of a band to the other, and a *drift* when $m = 0$ and the zone temperature floats.

Definition S6.5 (Schedule and infinite schedule). A *schedule* of horizon $t_{\max}$ is a finite sequence of timed actions $\sigma = \langle (m_1, t_1), \dots, (m_k, t_k) \rangle$ with $\sum_j t_j = t_{\max}$. An *infinite schedule* is either an infinite sequence $\langle (m_1, t_1), (m_2, t_2), \dots \rangle$ with $\sum_j t_j = \infty$, or a finite sequence whose last duration is $t_k = \infty$. Each unit follows its own schedule.

Definition S6.6 (Run, safe leap and safe schedule). The *run* of a schedule from the initial state $V^{(0)} = V_0$ is the sequence of states $V^{(0)}, V^{(1)}, V^{(2)}, \dots$ with $V^{(j)} = \Phi_{m_j}(V^{(j-1)}, t_j)$, the state reached by following the dynamics of mode m_j for time t_j from $V^{(j-1)}$; with constant rates, $V^{(j)} = V^{(j-1)} + t_j A(m_j)$. (The superscript indexes the run; the subscript i of V_i indexes zones. The labels $V_0, \dots, V_5$ of Fig. 4 are the states $V^{(0)}, \dots, V^{(5)}$ of one zone's run.) A timed action is a *safe leap* from a state if the trajectory stays in $\mathcal{S}$ for its whole duration. A schedule is *safe* if each of its timed actions is safe from the state its run has reached, and a safe schedule is *comfortable* if every conditioned zone also stays within the comfort band $[V_{\mathrm{low}}, V_{\mathrm{high}}] \subseteq \mathcal{S}$.

Definition S6.7 (Cost of a schedule). The cost of a finite schedule of unit i is $\pi(\sigma) = \sum_{j=1}^{k} \pi_i(m_j)\, t_j$. The cost of an infinite schedule is its limit-average cost

$$\pi_{\mathrm{avg}}(\sigma) = \limsup_{k \to \infty} \frac{\sum_{j=1}^{k} \pi_i(m_j)\, t_j}{\sum_{j=1}^{k} t_j},$$

and, for a finite sequence ending in (m_k, ∞), $\pi_{\mathrm{avg}}(\sigma) = \pi_i(m_k)$. Since $\pi_i(m)$ is the energy price λ times the electrical power, $\pi_{\mathrm{avg}} = \lambda J_\infty$, with J_∞ the long-run mean electrical power of the unit.

Definition S6.8 (Optimal leap). With the leap cycle, its level $\bar{V}$ and the condition $f_m \psi Q_i > L(\bar{V})$ under which mode m holds the zone as defined in Section 5.5, an *optimal leap* is a pair $(\bar{V}, m)$ whose mode holds the zone and whose cycle stays in the comfort band at the least cost π_{avg} (Fig. S1 shows the cycles of the running example). In the heating season the roles of drift and leap are reversed.

Definition S6.9 (Schedulability and utilisation). Following Alur et al. [14, 16], a zone is *safely schedulable* if it admits a safe infinite schedule. For states inside the safe set this holds if and only if there are dwell times whose rate vectors sum to zero over a period. For a single zone with drift rate $L/C_i > 0$ in mode 0 and rate $(L - f_m \psi Q_i)/C_i$ in mode m, this is the condition $f_m \psi Q_i > L$ of Section 5.5. The fraction of time the unit must spend in mode m, $d_m = L/(f_m \psi Q_i)$, is its *duty* in that mode, and the zone is schedulable in mode m if and only if $d_m < 1$. Over a leap cycle the *utilisation* $U_i = L/Q_i$ is the mean fraction of the unit's full capacity in use.

Remark S6.2. Nghiem et al. [18] give sufficient schedulability conditions for coupled zones that share a peak-power budget. Here no power budget is shared, so, as in Section 5.8, Definition S6.9 applies zone by zone.

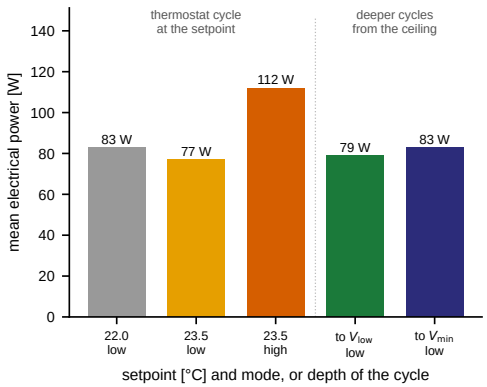


Fig. S1 Leap cycles of the running example (Bed 2 of apartment 2A, July, Riyadh).

Remark S6.3 (Why the cycle returns to the switching point). The run of Fig. 4 returns to the thermostat's lower switching point rather than descending to V_{low} or $V_{\min}$ in every cycle, because a deeper cycle holds the room colder on average and so admits more heat: as the running example of Section 6.2 shows.

S6.3 Heat budget of a passive zone

Proposition S6.1 (Heat budget of a passive zone). Let $u \in \mathcal{Z}_u$ be a passive zone and let overbars denote means over a period long compared with its time constant (a month), over which its stored heat changes negligibly. Then the heat that enters it balances the heat that leaves it:

$$\bar{q}_u^{\mathrm{env}} + \bar{G}_u + \bar{S}_u = \textstyle\sum_j K_{uj}(\bar{V}_u - \bar{V}_j) + \bar{D}_u, \qquad \text{(S1)}$$

where the left-hand side is the mean heat that enters from the outdoors, the ground and the zone's own gains, the sum is the heat it loses through walls and slabs, and $\bar{D}_u$ is the mean heat it loses through its open doorways. Consequently: (i) in the cooling season a passive zone with any exposure or gain is warmer than the conditioned rooms that take its heat; (ii) its temperature does not depend on the capacity of any unit, only on the temperatures the units hold; (iii) the more of its heat it sheds directly to conditioned rooms, through walls or open doors, the closer it stays to their setpoint; and (iv) passive zones that touch one another raise one another's temperature.

Proof. Averaging the heat balance of u (where no unit acts) over the period gives the change of its stored heat divided by the period on the left, which vanishes when the stored heat changes negligibly, and the mean of the right-hand side on the right. The conductive terms are linear in the temperatures with constant coefficients, so their means are the same expressions evaluated at the mean temperatures; the door term is kept as its mean $\bar{D}_u$. Setting the sum to zero gives Eq. (S1). In the cooling season the left-hand side is positive, so the right-hand side must be positive too; since both wall and door exchanges carry heat from warmer to cooler air, $\bar{V}_u$ must exceed the temperature of the rooms that receive its heat, which is (i). No unit capacity appears in Eq. (S1), which is (ii). For a given inflow, a larger share of exchange with rooms held at the setpoint requires a smaller excess $\bar{V}_u - \bar{V}_j$, which is (iii). A passive neighbour is itself warmer than the setpoint by (i), so heat shed to it requires a higher $\bar{V}_u$, which is (iv). It also follows that $\bar{V}_u$ is a weighted mean of its neighbours' and the outdoor and ground temperatures, which the proof of Theorem 1 (Section S2) uses. □

Running example (passive zones). In July in Riyadh ($\bar{T}_a = 36.4\,^{\circ}\mathrm{C}$) the bath beside the kitchen (Bath 4 in Table S3) of apartment 2A, with an exterior wall and a window, receives 127 W (80 W from the outdoors and 47 W of its own and solar gains). It sheds 22 W through its walls to conditioned rooms, 14 W to passive zones and 91 W through its open door, and averages $25.0\,^{\circ}\mathrm{C}$. The least exposed bath, the interior bath beside the maid room (Bath 2 in Table S3), receives only 36 W and averages $24.4\,^{\circ}\mathrm{C}$. By (i), each sits above the conditioned rooms that take its heat, and by (ii), a larger unit in a neighbouring room does not change that as long as the room is held at the same setpoint; Section S3 reports the passive zones of the whole building with and without the controller.

S6.4 Running example: further continuations

Coupled neighbours. Although Bed 2 is strongly coupled to its neighbours (Section 5.5), on the typical floor the zones on either side of the apartment's party and core walls differ by only 0.09 K on average over the year (Riyadh). Removing the coupling across those walls altogether changes the apartment's annual energy by 0.9%, and tripling it by -1.0%: a strong coupling carries little heat when no temperature difference drives it, as Section 6.1 states.

Free-floating room and the indoor COP factor. With its unit off, Bed 2 would float towards $43\,^{\circ}\mathrm{C}$ in mean July conditions: its insulated wall loses little, so its own and solar gains alone would hold it far above the ambient. The mean powers of the running example of Section 6 are evaluated without the indoor COP factor g ($\gamma = 0$); with it, every mean power would be about 8% higher at $23.5\,^{\circ}\mathrm{C}$ and 11% at $22\,^{\circ}\mathrm{C}$, which widens each difference.

Sources of saving. In July in Riyadh, Bed 2 gains 0.391 kW at $22\,^{\circ}\mathrm{C}$ and 0.363 kW at $23.5\,^{\circ}\mathrm{C}$: each kelvin of warmth admits about 19 W less heat, and its mean electrical power falls from 83 to 77 W (lever a of Proposition 3). Holding the same level in mode 3 would cost 112 W (lever b). Precooling the room admits the same 19 W per kelvin more, for as long as it lasts. Fig. S1 shows these mean powers, together with those of the deeper cycles that descend from the ceiling to V_{low} and to $V_{\min}$ in the lowest mode; both cost more than the thermostat cycle at $23.5\,^{\circ}\mathrm{C}$.

S7 Validation details

This appendix gives the details of the comparative tests of Section 8.2: the BESTEST-style test on the single-zone cases of Standard 140 and the settings of the storey-box comparison with EnergyPlus.

Table S4 BESTEST-style comparative test (Standard 140 cases on the Riyadh weather; differences computed from unrounded values): annual heating and cooling [MWh], peak hourly heating and cooling [kW], and the free-floating minimum, mean and maximum temperature [°C]. Cases 640/940: 600/900 with the night heating setback. E+: EnergyPlus 26.1; this: the engine of the model.

	Case 600		Case 900		Case 640		Case 940	
	E+	this	E+	this	E+	this	E+	this
Heating [MWh]	0.40	0.62	0.00	0.01	0.16	0.28	0.00	0.00
Cooling [MWh]	11.12	11.10	9.62	10.04	11.05	11.04	9.62	10.03
Peak heating [kW]	1.38	1.63	0.26	0.57	3.30	3.77	0.25	1.05
Peak cooling [kW]	6.57	5.83	4.02	3.60	6.57	5.83	4.02	3.60
	Case 600FF		Case 900FF					
Minimum [°C]	12.0	9.6	20.2	19.0				
Mean [°C]	39.1	37.9	39.2	37.9				
Maximum [°C]	71.1	65.6	51.6	47.1				

BESTEST-style comparative test. The engine of the model was run on the single-zone cases 600 (lightweight) and 900 (heavyweight) of Standard 140, with their geometry, constructions, 12 m^2 of south glazing, 200 W of internal gains, 0.5 ACH and the 20/27 °C setpoints, and with the units switched off (600FF and 900FF), on the Riyadh weather instead of the standard's Denver file. The same cases were run in EnergyPlus 26.1 (Table S4). This is a comparative test between two programs on the same inputs rather than the standard's acceptance test, whose reference ranges apply only to Denver. Cases 640 and 940 add the standard's night heating setback (10 °C from 23:00 to 07:00), which exercises the response of light and heavy construction to a setback. Free-floating, the mean temperature differs by -1.2 and -1.3 K and the annual maximum by -5.5 and -4.5 K. The engine therefore reproduces EnergyPlus's annual cooling closely but its peaks and extremes less closely: its exterior surfaces have a fixed film coefficient and no surface temperature of their own, and its structure is one node, so it damps the sharpest afternoon peaks. Heating is small in Riyadh, and its differences are a few hundred kWh.

Settings of the storey-box comparison. EnergyPlus runs with 10-minute time steps, its default conduction-transfer-function heat balance and surface convection algorithms, full exterior solar distribution and the same TMYx files as the model (Riyadh Air Base, WMO 404380, record 1958–2022; Jeddah King Abdulaziz International Airport, WMO 410240, record 1981–2025). On the storey box the internal gains of the two programs are identical and their infiltration gains differ by 2.1–12.5%. Their window solar gains are not defined alike: the engine's is the total solar heat gain through the SHGC, whereas the EnergyPlus output used is the transmitted solar radiation, which leaves out the absorbed share that flows inward; the engine's is 20–58% larger. The agreement in delivered cooling therefore does not show that every heat-gain component agrees, and part of it may come from compensating differences, such as the engine's fixed exterior film coefficient and one-node structure; the engine on the storey-box geometry finds an envelope effect of 53.6% in Riyadh and 53.0% in Jeddah, between those of EnergyPlus and of the room-resolved model.

S8 Full sensitivity analysis and pre-cooling robustness

This appendix gives the full one-at-a-time sensitivity analysis of Section 9.7 (Table 14 shows the decisive rows), the diagnostics behind it (sizing margin, controller resolution and humidity), the seasonal operation of the building, every test instance, and the stress tests of the pre-cooling result. All runs are of the whole building (Case 3); the sensitivity variants and the robustness tests are of the SBC-compliant building.

Every variant. For each of the 37 variants and both cities, the analysis gives the HVAC energy intensity, the setpoint lever, the best admissible pre-cool and the cost of a 2 K pre-peak pre-cool, as in the columns of Table 14. Over the zone-model variants the setpoint lever spans 8.0–12.6% and the 2 K pre-peak cost 1.8–6.7%; over the controller and COP-model variants the setpoint lever spans 8.1–14.0% and the 2 K pre-peak cost 2.0–5.1%; over the equipment variants the setpoint lever spans 8.8–12.8% and the 2 K pre-peak cost 2.1–5.2%; over the envelope and air variants the setpoint lever spans 9.5–17.0% and the 2 K pre-peak cost 3.1–4.6%; over the weather variants the setpoint lever spans 9.7–12.2% and the 2 K pre-peak cost 3.1–4.6%. The setpoint lever is largest in the variant "ground slab without soil resistance, constant ground temperature" (17.0%, Riyadh) and smallest in the variant "one node, COP independent of indoor air" (8.0%, Jeddah); the pre-peak cost is largest in the variant "one node per zone" (6.7%, Jeddah) and smallest in the variant "one node, COP independent of indoor air" (1.8%, Riyadh). The ground variant is a bound on ground coupling rather than an alternative estimate: it replaces the ISO 13370 slab transmittance (0.40 W/m^2K) by the U-value of the slab alone (2.77), without the soil resistance, and the monthly ground temperature by a constant 26 °C in Riyadh and 29 °C in Jeddah, close to the annual means of the record. The ground floor then gains heat from the warm soil all year, which raises Jeddah's HVAC energy intensity to 42.2 kWh/m^2yr and Riyadh's setpoint lever to 17.0%, while no pre-cooling setting saves. The HVAC energy intensity of the admissible variants spans 20.9–33.4 in Riyadh and 30.4–52.4 kWh/m^2yr in Jeddah. The variant "sized by load with a 15% margin" is inadmissible (Section 9.7).

Sizing margin. Units sized by load are sized at a multiple of each room's peak hourly load on the sampled days; of the margins tried in turn (1.15, 1.5, 2, 2.5), the first at which every room stays within the safe set is 2.5 in both cities. A finer sweep of the margin (1.15, 1.25, 1.5, 1.75, 2, 2.5, 3) shows what it buys. At the margins that keep every room within the safe set (2.5, 3) the units save 15.5–16.5% in Riyadh and 10.6–11.2% in Jeddah against the catalogue units; the smaller margins are inadmissible, and only their excursion is reported: it falls from 69 K·h in Riyadh and 18 K·h in Jeddah at 1.15 to zero from 2.5 on, so the smallest margin that keeps every room within the safe set lies between 2 and 2.5. Every unit is at the 0.75-ton minimum size at 1.15, so the building needs 45 tons at 1.15 and 63–66 at 3: in capacity the margins differ far less than their names suggest. The excursions are small (the warmest room peaks at 24.15 °C) and occur mostly in the guest rooms (98–100% of the excursion at the tightest margin). As in the hard instances of Section 9.5, they arise while a running unit escalates from a lower mode, not at start-up; Sections 9.5 and 10.3 discuss what this implies for the margin. The change of compressor, which the 3-ton variant measures on its own, accounts for most of the difference between the units sized by load as inverter units (16.5% in Riyadh and 11.2% in Jeddah against the catalogue units) and with the fixed-speed zones keeping fixed-speed units (2.1% in Riyadh and 0.2% in Jeddah), although the two effects are not additive.

Controller resolution. The units start on average 2.0 (Riyadh) and 2.6 (Jeddah) times per hour of the year, a rate set by the 3-minute time step rather than by a measured cycle; without the 3-minute restart delay the bill changes by less than 0.01%. The twelve fixed-speed 3-ton units run 3–6% of the time and, as inverter units, would use 39% less; the four stair units, a feature of the building studied rather than of every Saudi apartment block, take 8.9–9.1% of the units' electricity and are billed to the common meter. The robustness tests below show how far a 1-minute step, minimum on- and off-times and a cycling loss charged per start move the results.

Humidity. The main model prices the latent load at a fixed latent COP and assumes the indoor target is met. A diagnostic humidity balance per zone tests that assumption: moisture enters with infiltration and from five occupants per dwelling, and the coil removes it at a given sensible heat ratio while the unit runs. In Riyadh the target holds: the conditioned rooms exceed 60% relative humidity in 0.8% of the cooling-season hours. In Jeddah the sensible runtime of the oversized units is too short: at a sensible heat ratio of 0.75 the rooms exceed 60% in 41% of the hours (21% at 0.65), and the coil removes 82% of the latent load, so holding the target needs dedicated dehumidification, whose electricity the latent term prices. Internal latent gains would add 0.2% (Riyadh) and 3.2% (Jeddah) to the HVAC energy under every schedule, leaving every absolute saving unchanged. A 30% lower latent COP whenever the units are off or in the lowest mode raises Jeddah's latent share to 33% and leaves the scheduling result unchanged. Run for the levers themselves (current practice, the reference setpoint and 2 K of pre-peak or night pre-cooling), the diagnostic hardly moves: at a sensible heat ratio of 0.75 the rooms exceed 60% in 0.7–0.9% of the cooling-season hours in Riyadh and 41.1–44.6% in Jeddah. At that ratio the higher setpoint lowers the Jeddah share slightly, since warmer air holds the same moisture at a lower relative humidity, while at 0.65 it raises it by 1.3 percentage points. Pre-peak pre-cooling raises it at both ratios, the coil then removing 76% of the latent load instead of 82%. The setpoint lever therefore costs little humidity comfort and pre-cooling gains none.

Table S5 Summer and winter operation of the whole building at the reference policy: annual cooling, heating and latent electricity [kWh], and the share of time [%] the units of the conditioned rooms spend off and in the low, medium and high modes, given as off/low/medium/high (cooling and heating together; fixed-speed units count as high) in summer (Jun–Sep) and winter (Dec–Feb). The remainder of the HVAC energy is the units' standby electricity, 1,577 kWh a year in the SBC-compliant building. Last row: summer / winter shares of apartment 2A's HVAC energy.

	Riyadh		Jeddah	
	SBC	Pre-code	SBC	Pre-code
Cooling [kWh]	47,383	103,038	54,784	116,870
Heating [kWh]	1,367	11,116	0	0
Latent [kWh]	185	185	19,551	19,551
Summer modes [%]	59/33/1/7	40/32/15/13	63/31/0/6	44/32/13/12
Winter modes [%]	97/2/0/1	81/14/1/5	82/14/0/4	75/18/2/6
Apt. 2A summer/winter [%]	61.0/3.9	–	46.8/12.6	–

Seasonal operation. The model runs through the whole year with units that cool and heat (Table S5). In Riyadh summer accounts for 61% of apartment 2A's HVAC energy and winter for 4%; Jeddah spreads its load more evenly (47% and 13%). The SBC-compliant building needs little heating (Section 9.2), because its internal gains and its neighbours keep most rooms above the heating setpoint. At the reference policy no conditioned room of the SBC-compliant building leaves the safe set in either season (cold excursion 0 K · h in both cities). Over the year the units of the SBC-compliant building run in the medium or high mode in 4.5–5.2% of the hours, the fixed-speed units, which run only at full capacity, counted as high (Table S5).

Test instances. Table 13 reports the eight instances with the catalogue units in one row, with their ranges, and the four hard instances one by one. With the catalogue units, the HVAC energy intensity (ranges over the two cities) is 25.1–37.7 (SBC, TMYx), 32.5–46.0 (SBC, heat wave), 57.5–68.5 (pre-code, TMYx) and 72.2–89.1 (pre-code, heat wave) kWh/m^{2}yr, and the peak load ratio is 0.19–0.26 (SBC) and 0.53–0.62 (pre-code). Of the 49 lattice policies, all 49 are admissible in the SBC building and 30–42 in the pre-code building, and the best is no pre-cooling in all eight. The four tightly sized instances have peak load ratios of 0.58, 0.57, 0.79 and 0.75 (SBC Riyadh, SBC Jeddah, pre-code Riyadh, pre-code Jeddah), an annual excursion above the ceiling of 68.6, 17.8, 81.2 and 28.7 K·h in the same order, a warmest room of at most 24.2 °C, no admissible lattice policy, and an HVAC energy intensity 13.3–19.5% below that of the

Table S6 Robustness of the thermostat pre-cooling result (SBC-compliant building, Case 3, volume tariff). Best: saving of the cheapest admissible policy against no pre-cooling [%] (positive: saves; 0: no pre-cooling is best; negative: every depth run costs, for the rows that do not include no pre-cooling among their options; –: not run, or inadmissible because the reference policy leaves the safe set). 2 K: change in the annual bill of a 2 K pre-peak pre-cool [%] (positive: costs). Favourable choices: one node per zone, COP independent of the indoor air, inverter units in their lowest mode, no cycling loss. Dawn setback: all 365 days; the other rows: sampled year.

	Riyadh		Jeddah	
Test	Best	2 K	Best	2 K
Base model, lattice of 49 policies	+0.00	+3.40	+0.00	+4.30
Inverter units in lowest mode	+0.00	+1.95	+0.00	+2.84
Ramped pre-peak setback (0.5 K/h)	−0.25	+2.26	−0.34	+3.04
Extra heat scaled to EnergyPlus	–	+2.94	–	+3.82
Dawn setback, 2 K, all 365 days	−0.99	–	−1.80	–
Top floor only (15 units)	+0.00	+0.82	+0.00	+1.14
Rooms with west windows only (12 units)	+0.00	+1.02	+0.00	+1.29
Cycling loss charged per start	+0.00	+2.45	+0.00	+2.82
1-minute step	+0.00	+2.11	+0.00	+2.85
1-minute step, 3-min minimum on/off, loss per start	–	–	+0.00	+2.45
Favourable choices combined	+0.77	−0.21	+0.03	+3.07
Favourable choices, top floor only	+0.21	−0.20	+0.00	+0.50

catalogue units; at 23 °C every one of them is admissible.

Robustness of the pre-cooling result. Table S6 collects these stress tests (SBC-compliant building, Case 3). None of them saves, except the favourable combinations, which need every favourable choice at once and save at most 0.77%. The loss per start is the unit's full power for 1.5 min at each start of a fixed-speed unit and for 0.82 min at each start of an inverter unit, calibrated to the part-load factor at the cyclic rating point; the controller variants move the absolute bill by 2–32%, the loss per start most, but not the sign of pre-cooling. With minimum on- and off-times the variant is inadmissible in Riyadh: its reference policy exceeds the ceiling from December to February, within the heating months (November to March), when the oversized fixed-speed units, held on for 3 minutes while heating, overshoot it (636 K·h a year). The scaling to EnergyPlus multiplies the heat term of each 2 K run of Table 9 by the ratio r of the extra heat that EnergyPlus and the engine find for the same setback on the storey box (Table 4; r is 0.75–0.83) and holds the change in mean COP, so that a bill change $\Delta\Pi$ with a heat change ΔH becomes $(1+\Delta\Pi)(1+r\Delta H)/(1+\Delta H)-1$. Scaled in this way, a 2 K night pre-cool still costs 3.2% in Riyadh and 3.3% in Jeddah. With the favourable choices combined, the best ramped setback lowers the bill by 0.55% in Riyadh and raises it by 0.29% in Jeddah; with the 0.08% of the one-node variant whose COP ignores the room temperature (Table 14), these rows hold the only savings found for thermostat pre-cooling. No policy cools a room of the SBC-compliant building below the 20 °C floor; in the pre-code building, on the sampled days, 7 (Riyadh) and 13 (Jeddah) of the 49 policies are inadmissible and are excluded. Of these, 7 in Jeddah let rooms drift below the floor on cool nights, by at most 0.2 K·h a year and to 19.9 °C, and the remaining 7 in Riyadh and 6 in Jeddah pass the ceiling. The cheapest admissible policy remains no pre-cooling.

Table S7 Inputs of the uncertainty analysis: base value and uniform range.

Input	Base	Low	High
indoor COP slope γ	0.02	0	0.03
outdoor COP slope	0.02	0.01	0.03
COP ratio c_1/c_3	1.45	1.3	1.6
COP ratio c_2/c_3	1.24	1.1	1.3
inverter C_d	0.15	0.05	0.25
fixed-speed C_d	0.25	0.15	0.35
escalation-threshold scale	1	0.5	2
air-node share of capacitance	0.05	0.02	0.15
latent COP	3.4	2.5	4
infiltration	0.4	0.2	0.8
internal-gain scale	1	0.7	1.3
wall U (thermal bridges)	1	1	1.2
opaque solar absorptance	0.7	0.5	0.9
door exchange (scale)	1	0.5	1.5
capacity derating slope	0.01	0.005	0.02
daily temperature swing (scale)	1	0.8	1.3
air temperature shift [K]	0	−1	2

S9 Uncertainty analysis

Seventeen assumed inputs of the SBC-compliant building (Case 3, sampled year) are varied jointly over the uniform ranges of Table S7 by a Latin hypercube of 128 samples per city (fixed seed). This appendix gives the input ranges and the partial rank correlations. For each sample the reference, current-practice and 0.5–2 K pre-cooling policies (night or pre-peak), the pre-code building and the 3-ton units as inverter units are simulated. The weather inputs scale the daily swing of the air temperature about each day's mean and shift it uniformly (the heating months follow the shifted weather). The strongest partial rank correlations (Riyadh/Jeddah, ranked by the larger magnitude of the two) are as follows. For the setpoint lever they are the indoor COP slope γ (+0.93/+0.98), the infiltration (−0.85/−0.57) and the latent COP (−0.10/+0.84). For the envelope lever they are the infiltration (−0.88/−0.96), the internal-gain scale (−0.90/−0.77) and the opaque solar absorptance (+0.85/+0.87). For the inverter lever they are the fixed-speed C_d (+0.94/+0.95), the COP ratio c_1/c_3 (+0.90/+0.89) and the inverter C_d (−0.89/−0.89). For the cost of a 2 K pre-peak pre-cool they are the indoor COP slope γ (+0.69/+0.65), the air-node share of capacitance (−0.44/−0.46) and the inverter C_d (−0.37/−0.38). For the cost of a 2 K night pre-cool they are the indoor COP slope γ (+0.76/+0.81), the outdoor COP slope (−0.78/−0.80) and the infiltration (+0.55/+0.15). The best admissible pre-cool is zero in every sample and so has no rank correlation.

References

[1] Moncef Krarti, Mohammad Aldubyan, and Eric Williams. Residential building stock model for evaluating energy retrofit programs in Saudi Arabia. *Energy*, 195:116980, 2020. https://doi.org/10.1016/j.energy.2020.116980.

[2] Lucelia Rodrigues, Benjamin A. Cherian, and Serik Tokbolat. Reducing cooling energy demand in Saudi Arabian residential buildings using passive design approaches. *Buildings*, 15(11): 1895, 2025. https://doi.org/10.3390/buildings15111895.

[3] Ahmed Felimban, Ulrich Knaack, and Thaleia Konstantinou. Evaluating savings potentials using energy retrofitting measures for a residential building in Jeddah, KSA. *Buildings*, 13 (7):1645, 2023. https://doi.org/10.3390/buildings13071645.

[4] James E. Braun. Reducing energy costs and peak electrical demand through optimal control of building thermal storage. *ASHRAE Transactions*, 96(2):876–887, 1990.

[5] Shayan Naderi, Gloria Pignatta, Simon Heslop, Iain MacGill, and Dong Chen. Demand response via pre-cooling and solar pre-cooling: a review. *Energy and Buildings*, 272:112340, 2022. https://doi.org/10.1016/j.enbuild.2022.112340.

[6] Stepp Mayes, Tong Zhang, and Kelly T. Sanders. Residential precooling on a high-solar grid: impacts on CO_2 emissions, peak period demand, and electricity costs across California. *Environmental Research: Energy*, 1(1):015001, 2024. https://doi.org/10.1088/2753-3751/acfa91.

[7] Saudi Electricity Regulatory Authority. Consumption Tariff. https://www.sera.gov.sa/en/consumer/electric-tariff/electric-tariff-categories/consumption-tariff, 2026. Residential: 0.18 SAR/kWh up to 6000 kWh per month, 0.30 SAR/kWh above; bills subject to 15% VAT; accessed 25 September 2026.

[8] Hamzah Faraj. Cost-effective tariff-aware HVAC coordination in Saudi residential buildings using physics-informed deep reinforcement learning. *Journal of King Saud University – Engineering Sciences*, 38(7):58, 2026. https://doi.org/10.1007/s44444-026-00131-0.

[9] Jérôme Le Dréau and Per Heiselberg. Energy flexibility of residential buildings using short term heat storage in the thermal mass. *Energy*, 111:991–1002, 2016. https://doi.org/10.1016/j.energy.2016.05.076.

[10] Glenn Reynders, Rui Amaral Lopes, Anna Marszal-Pomianowska, Daniel Aelenei, João Martins, and Dirk Saelens. Energy flexible buildings: an evaluation of definitions and quantification methodologies applied to thermal storage. *Energy and Buildings*, 166:372–390, 2018. https://doi.org/10.1016/j.enbuild.2018.02.040.

[11] Mahmoud A. A. Mousa, Sven Schewe, and Dominik Wojtczak. Optimal control for simple linear hybrid systems. In *2016 23rd International Symposium on Temporal Representation and Reasoning (TIME)*, pages 12–20. IEEE, 2016. https://doi.org/10.1109/TIME.2016.9.

[12] Mahmoud A. A. Mousa, Sven Schewe, and Dominik Wojtczak. Optimal control for multi-mode systems with discrete costs. In *Formal Modeling and Analysis of Timed Systems (FORMATS 2017)*, volume 10419 of *Lecture Notes in Computer Science*, pages 77–96. Springer, 2017. https://doi.org/10.1007/978-3-319-65765-3_5.

[13] Thomas A. Henzinger. The theory of hybrid automata. In *Verification of Digital and Hybrid Systems*, pages 265–292. Springer, 2000. https://doi.org/10.1007/978-3-642-59615-5_13.

[14] Rajeev Alur, Ashutosh Trivedi, and Dominik Wojtczak. Optimal scheduling for constant-rate multi-mode systems. In *Proceedings of the 15th ACM international conference on Hybrid Systems: Computation and Control*, pages 75–84. ACM, 2012. https://doi.org/10.1145/2185632.2185647.

[15] Dominik Wojtczak. Optimal control for linear-rate multi-mode systems. In *Formal Modeling and Analysis of Timed Systems (FORMATS 2013)*, volume 8053 of *Lecture Notes in Computer Science*, pages 258–273. Springer, 2013. https://doi.org/10.1007/978-3-642-40229-6_18.

[16] Rajeev Alur, Vojtěch Forejt, Salar Moarref, and Ashutosh Trivedi. Safe schedulability of bounded-rate multi-mode systems. In *Proceedings of the 16th International Conference on Hybrid Systems: Computation and Control (HSCC)*, pages 243–252. ACM, 2013. https://doi.org/10.1145/2461328.2461366.

[17] Truong X. Nghiem, Madhur Behl, Rahul Mangharam, and George J. Pappas. Green scheduling of control systems for peak demand reduction. In *Proceedings of the 50th IEEE Conference on Decision and Control and European Control Conference (CDC-ECC)*, pages 5131–5136. IEEE, 2011. https://doi.org/10.1109/CDC.2011.6161164.

[18] Truong X. Nghiem, Madhur Behl, Rahul Mangharam, and George J. Pappas. Scalable scheduling of building control systems for peak demand reduction. In *Proceedings of the American Control Conference (ACC)*, pages 3050–3055. IEEE, 2012. https://doi.org/10.1109/ACC.2012.6315252.

[19] Ján Drgoňa, Javier Arroyo, Iago Cupeiro Figueroa, David Blum, Krzysztof Arendt, Donghun Kim, Enric Perarnau Ollé, Juraj Oravec, Michael Wetter, Draguna L. Vrabie, and Lieve Helsen. All you need to know about model predictive control for buildings. *Annual Reviews in Control*, 50:190–232, 2020. https://doi.org/10.1016/j.arcontrol.2020.09.001.

[20] Dongsu Kim, Jongman Lee, Sunglok Do, Pedro J. Mago, Kwang Ho Lee, and Heejin Cho. Energy modeling and model predictive control for HVAC in buildings: A review of current research trends. *Energies*, 15(19):7231, 2022. https://doi.org/10.3390/en15197231.

[21] Juan Hou, Haoran Li, Natasa Nord, and Gongsheng Huang. Model predictive control under weather forecast uncertainty for HVAC systems in university buildings. *Energy and Buildings*, 257:111793, 2022. https://doi.org/10.1016/j.enbuild.2021.111793.

[22] Grace Dhaliwal, Burak Gunay, and Ian Beausoleil-Morrison. Parametric analysis of model predictive control for residential HVAC systems. *Energy and Buildings*, 351:116662, 2026. https://doi.org/10.1016/j.enbuild.2025.116662.

[23] Wanfu Zheng, Dan Wang, and Zhe Wang. Economic model predictive control for building HVAC system: a comparative analysis of model-based and data-driven approaches using the BOPTEST framework. *Applied Energy*, 374:123969, 2024. https://doi.org/10.1016/j.apenergy.2024.123969.

[24] Huilong Wang, Daran Mai, Qian Li, and Zhikun Ding. Evaluating machine learning models for HVAC demand response: the impact of prediction accuracy on model predictive control performance. *Buildings*, 14(7):2212, 2024. https://doi.org/10.3390/buildings14072212.

[25] W. J. N. Turner, I. S. Walker, and J. Roux. Peak load reductions: Electric load shifting with mechanical pre-cooling of residential buildings with low thermal mass. *Energy*, 82:1057–1067, 2015. https://doi.org/10.1016/j.energy.2015.02.011.

[26] Jiewei Wang, Ziqing Wei, Yikang Zhu, Chunyuan Zheng, Bin Li, and Xiaoqiang Zhai. Demand response via optimal pre-cooling combined with temperature reset strategy for air conditioning system: A case study of office building. *Energy*, 282:128751, 2023. https://doi.org/10.1016/j.energy.2023.128751.

[27] James E. Braun. Load control using building thermal mass.

Journal of Solar Energy Engineering, 125(3):292–301, 2003. https://doi.org/10.1115/1.1592184.

[28] Stephen Morgan and Moncef Krarti. Impact of electricity rate structures on energy cost savings of pre-cooling controls for office buildings. *Building and Environment*, 42(8):2810–2818, 2007. https://doi.org/10.1016/j.buildenv.2005.11.010.

[29] Alexandre Canet and Meysam Qadrdan. Quantification of flexibility from the thermal mass of residential buildings in England and Wales. *Applied Energy*, 349:121616, 2023. https://doi.org/10.1016/j.apenergy.2023.121616.

[30] Reza Arababadi, Mohamed Elzomor, and Kristen Parrish. Selection of energy efficiency measures to enhance the effectiveness of pre-cooling in residential buildings in hot arid climate. *Science and Technology for the Built Environment*, 23(5):858–867, 2017. https://doi.org/10.1080/23744731.2016.1262660.

[31] José Adrián Rama Curiel and Jagruti Thakur. A novel approach for direct load control of residential air conditioners for demand side management in developing regions. *Energy*, 258:124763, 2022. https://doi.org/10.1016/j.energy.2022.124763.

[32] Frauke Oldewurtel, Andreas Ulbig, Alessandra Parisio, Göran Andersson, and Manfred Morari. Reducing peak electricity demand in building climate control using real-time pricing and model predictive control. In *49th IEEE Conference on Decision and Control (CDC)*, pages 1927–1932. IEEE, 2010. https://doi.org/10.1109/CDC.2010.5717458.

[33] Walid Matar. A look at the response of households to time-of-use electricity pricing in Saudi Arabia and its impact on the wider economy. *Energy Strategy Reviews*, 16:13–23, 2017. https://doi.org/10.1016/j.esr.2017.02.002.

[34] Essam Alayed, Richard O'Hegarty, and Oliver Kinnane. Thermal envelope analysis for new code compliance of Saudi Arabian dwellings. *Energy and Buildings*, 243:110997, 2021. https://doi.org/10.1016/j.enbuild.2021.110997.

[35] Saleh H. Alyami, Ali Alqahtany, Noman Ashraf, Abdelbagi Osman, Naief Ali Aldossary, Ayman Almutlaqa, Faris Al-Maziad, Maher S. Alshammari, and Wadee Ahmed Ghanem Al-Gehlani. Impact of location and insulation material on energy performance of residential buildings as per Saudi Building Code (SBC) 601/602 in Saudi Arabia. *Materials*, 15(24):9079, 2022. https://doi.org/10.3390/ma15249079.

[36] Mana Alyami and Siddig Omer. Building energy performance simulation: a case study of modelling an existing residential building in Saudi Arabia. *Environmental Research: Infrastructure and Sustainability*, 1(3):035001, 2021. https://doi.org/10.1088/2634-4505/ac241e.

[37] Ahmed Felimban, Alejandro Prieto, Ulrich Knaack, Tillmann Klein, and Yasser Qaffas. Assessment of current energy consumption in residential buildings in Jeddah, Saudi Arabia. *Buildings*, 9(7):163, 2019. https://doi.org/10.3390/buildings9070163.

[38] Mohammad S. Al-Homoud and Moncef Krarti. Energy efficiency of residential buildings in the Kingdom of Saudi Arabia: Review of status and future roadmap. *Journal of Building Engineering*, 36:102143, 2021. https://doi.org/10.1016/j.jobe.2020.102143.

[39] Moncef Krarti and Mohammad Aldubyan. Peak demand-based optimization approach for building retrofits: case study of Saudi residential buildings. *Energy Efficiency*, 15(8):69, 2022. https://doi.org/10.1007/s12053-022-10077-2.

[40] Alaa Alaidroos and Moncef Krarti. Optimal design of residential building envelope systems in the Kingdom of Saudi Arabia. *Energy and Buildings*, 86:104–117, 2015. https://doi.org/10.1016/j.enbuild.2014.09.083.

[41] Moncef Krarti and Nicholas Howarth. Transitioning to high efficiency air conditioning in Saudi Arabia: a benefit cost analysis for residential buildings. *Journal of Building Engineering*, 31:101457, 2020. https://doi.org/10.1016/j.jobe.2020.101457.

[42] Ahmed Almogbel, Fahad Alkasmoul, Zaid Aldawsari, Jaber Alsulami, and Ahmed Alsuwailem. Comparison of energy consumption between non-inverter and inverter-type air conditioner in Saudi Arabia. *Energy Transitions*, 4(2):191–197, 2020. https://doi.org/10.1007/s41825-020-00033-y.

[43] Mohammad Aldubyan and Moncef Krarti. Impact of stay home living on energy demand of residential buildings: Saudi Arabian case study. *Energy*, 238:121637, 2022. https://doi.org/10.1016/j.energy.2021.121637.

[44] Jubran Alshahrani and Peter Boait. Reducing high energy demand associated with air-conditioning needs in Saudi Arabia. *Energies*, 12(1):87, 2019. https://doi.org/10.3390/en12010087.

[45] Tyler Hoyt, Edward Arens, and Hui Zhang. Extending air temperature setpoints: simulated energy savings and design considerations for new and retrofit buildings. *Building and Environment*, 88:89–96, 2015. https://doi.org/10.1016/j.buildenv.2014.09.010.

[46] ASHRAE. ANSI/ASHRAE Standard 55-2023: Thermal Environmental Conditions for Human Occupancy. American Society of Heating, Refrigerating and Air-Conditioning Engineers, Peachtree Corners, GA, 2023.

[47] International Organization for Standardization. ISO 7730:2025 – Ergonomics of the Thermal Environment: Analytical Determination and Interpretation of Thermal Comfort Using Calculation of the PMV and PPD Indices and Local Thermal Comfort Criteria. ISO, Geneva, 2025.

[48] Kahramaa. Qatar General Electricity and Water Corporation (Kahramaa), National Program for Conservation and Energy Efficiency (Tarsheed). Tips to Using an Air Conditioner Efficiently. https://www.km.qa/Tarsheed/Pages/TarsheedDetails.aspx?ItemID=2, 2026. Accessed 7 October 2026.

[49] Saudi Building Code National Committee. *Saudi Building Code: General Building Code (SBC 201), Section 1010: Doors, Gates and Turnstiles*. Saudi Building Code National Committee, Riyadh, Saudi Arabia, 2018.

[50] Saudi Standards, Metrology and Quality Organization (SASO). SASO 2663:2014 – Energy Labelling and Minimum Energy Performance Requirements for Air-Conditioners. Policy record: https://www.iea.org/policies/2429-saso-26632014-meps-and-labelling-for-air-conditioners, 2014. Minimum EER of 11.5 (Btu/h)/W at test condition T1 for split units from 2015.

[51] Saudi Standards, Metrology and Quality Organization (SASO). SASO 2663:2021 – Air Conditioners: Minimum Energy Performance, Labelling and Testing Requirements for Low Capacity Window and Single-Split Types. Policy record: https://www.iea.org/policies/20488-saso-26632021-standard-for-air-conditioners, 2021. Replaces SASO 2663:2018; introduces the Seasonal Energy Efficiency Ratio (SEER).

[52] Saudi Building Code National Committee. *Saudi Building Code: Saudi Energy Conservation Code for Low-Rise Resi-*

dential Buildings (SBC 602). Saudi Building Code National Committee, Riyadh, Saudi Arabia, 2018.

[53] International Organization for Standardization. ISO 13370:2017 – Thermal Performance of Buildings: Heat Transfer via the Ground: Calculation Methods. ISO, Geneva, 2017.

[54] International Organization for Standardization. ISO 13790:2008 – Energy Performance of Buildings: Calculation of Energy Use for Space Heating and Cooling. ISO, Geneva, 2008. Withdrawn; superseded by ISO 52016-1:2017.

[55] W. G. Brown and K. R. Solvason. Natural convection through rectangular openings in partitions—1: Vertical partitions. *International Journal of Heat and Mass Transfer*, 5(9):859–868, 1962. https://doi.org/10.1016/0017-9310(62)90184-9.

[56] ASHRAE. ASHRAE Handbook – Fundamentals (SI Edition). ASHRAE, Peachtree Corners, GA, 2021.

[57] Air-Conditioning, Heating, and Refrigeration Institute. AHRI Standard 210/240-2017: Performance Rating of Unitary Air-Conditioning & Air-Source Heat Pump Equipment. AHRI, Arlington, VA, 2017.

[58] Saudi Energy. Saudi Energy announces electricity service tariff adjustment from January 1, 2027. Saudi Press Agency (SPA), Riyadh, 25 October 2026, https://www.spa.gov.sa/en/N2709801, 2026. Tariff details: https://www.se.com.sa/ar-SA/ourservices/columnc/bills-and-consumption/consumptiontariffs/ct2/ct2. Residential: 0.21 SAR/kWh up to 6000 kWh per month, 0.33 SAR/kWh above, excluding VAT; fixed monthly charge 70–100 SAR by breaker capacity; accessed 26 October 2026.

[59] Drury B. Crawley, Linda K. Lawrie, Frederick C. Winkelmann, W. F. Buhl, Y. Joe Huang, Curtis O. Pedersen, Richard K. Strand, Richard J. Liesen, Daniel E. Fisher, Michael J. Witte, and Jason Glazer. EnergyPlus: creating a new-generation building energy simulation program. *Energy and Buildings*, 33(4):319–331, 2001. https://doi.org/10.1016/S0378-7788(00)00114-6.

[60] Lukas Schork and Jacek Gondzio. Implementation of an interior point method with basis preconditioning. *Mathematical Programming Computation*, 12(4):603–635, 2020. https://doi.org/10.1007/s12532-020-00181-8.

[61] Q. Huangfu and J. A. J. Hall. Parallelizing the dual revised simplex method. *Mathematical Programming Computation*, 10(1):119–142, 2018. https://doi.org/10.1007/s12532-017-0130-5.

[62] Paul J. Goulart and Yuwen Chen. Clarabel: An interior-point solver for conic programs with quadratic objectives. *Mathematical Programming Computation*, 2026. https://doi.org/10.1007/s12532-026-00320-7. Online first, 21 May 2026.

[63] J. C. Helton and F. J. Davis. Latin hypercube sampling and the propagation of uncertainty in analyses of complex systems. *Reliability Engineering & System Safety*, 81(1):23–69, 2003. https://doi.org/10.1016/S0951-8320(03)00058-9.

[64] Simeone Marino, Ian B. Hogue, Christian J. Ray, and Denise E. Kirschner. A methodology for performing global uncertainty and sensitivity analysis in systems biology. *Journal of Theoretical Biology*, 254(1):178–196, 2008. https://doi.org/10.1016/j.jtbi.2008.04.011.

[65] Wei Tian. A review of sensitivity analysis methods in building energy analysis. *Renewable and Sustainable Energy Reviews*, 20:411–419, 2013. https://doi.org/10.1016/j.rser.2012.12.014.

[66] Andrea Saltelli and Paola Annoni. How to avoid a perfunctory sensitivity analysis. *Environmental Modelling & Software*, 25 (12):1508–1517, 2010. https://doi.org/10.1016/j.envsoft.2010.04.012.

[67] Ron Judkoff and Joel Neymark. Model validation and testing: The methodological foundation of ASHRAE Standard 140. *ASHRAE Transactions*, 112(2):367–376, 2006.

[68] ASHRAE. ANSI/ASHRAE Standard 140-2023: Method of Test for Evaluating Building Performance Simulation Software. American Society of Heating, Refrigerating and Air-Conditioning Engineers, Peachtree Corners, GA, 2023.

[69] Sh. Mahmoud, Y. Alyousef, Y. Alusaimi, I. Yassin, and A. Alelwan. Time-of-use tariff program in Saudi Arabia: Design, implementation, and evaluation. *Journal of King Saud University - Engineering Sciences*, 22(2):165–172, 2010. https://doi.org/10.1016/S1018-3639(18)30503-8.